University of Washington Nuclear Physics Laboratory

Energy loss in thin layers of argon.

Hans Bichsel
Telephone: 206-329-2792, FAX: 206-685-4634
e-mail: bichsel@gluon.npl.washington.edu
Nuclear Physics Laboratory 354290
University of Washington
Seattle, WA 98195-4290

March 19, 2000

Ultrarelativistic Heavy Ions Group

gluon::[bichsel]argo76.tex 09:30 19.3.2000

I. Introduction.

During my visit at BNL for the commissioning run of RHIC in July 1999, I discussed aspects of particle identification ("PID") in the time-projection-chamber ("TPC") with several people. One of the problems we perceived was the peculiar shape of the straggling function for very thin layers of gas. I have calculated some of these functions and want to explain the shapes.

I define as a track the ionization trace left by the passage of a charged particle through the TPC. A track consists of segments with lengths x along which the ionization is measured. Here I want to describe only the energy loss in single segments. It is defined by the straggling function $f(x, \Delta)$, where $\Delta = \sum_i E_i$ is the sum of discrete single energy losses E_i of the particles in a thickness x. Other aspects will be considered in later papers.

It must be kept in mind that the energy loss by the particle will differ from the energy deposition in the gas because some δ rays may have sufficient energy to escape into a neighboring gas volume. The effect is most important in the direction perpendicular to the track [1]. Energy deposition is not considered in this note.

As an example, the energy loss of particles with charge 1 and $\beta\gamma = 4.48$ (625 MeV/c pions) is given. The gas is assumed to be argon at 1 atm. Problems in constructing single collision spectra are discussed. The change due to the addition of methane in P-10 will be considered elsewhere.

II. Calculation of single collision spectrum $f(E)$.

A convenient way of calculating energy loss straggling functions is the convolution method [2, 3, 4, 5]. The initial function needed for this is the differential cross section $\sigma(E, \beta)$ for an energy loss E in collisions of particles (with charge ze and speed β) with argon atoms. This function is called the *single collision spectrum* [3, 5]. It is essentially the same as that used in GEANT in 1999 [6], but the convolution method used here gives smooth straggling functions $f(\Delta)$ which correspond to an infinite number of particles, rather than the stochastic results $f_G(\Delta)$ from GEANT, or from an experiment. Thus features due to the inherent structure of $\sigma(E, \beta)$ can clearly be discerned in the resulting functions.

In principle, the doubly differential cross section $\sigma(E, p, \beta)$ for a collision with energy loss E and momentum transfer p to the atom should be used. Usually, most of this energy and momentum will be given to the secondary electron. $\sigma(E, p, \beta)$ can be calculated with the Bethe-GOS (generalized oscillator strength) method, section 87.3.3 in [7]. At present, GOS for Ar is not available (GOS functions for Si are available [3]).

Therefore, the collision spectrum here instead is calculated with the Fermi-virtual-photon method (FVP or PAI) section 87.3.4 in [7], for which the photo absorption spectrum $\phi(hf)$ [8, 9] is needed. In PAI, the GOS is approximated (Fig. 87.4 in [7]) by a constant value between the possible minimum momentum transfer and $p_E^2 = 2E/m$, where m is the electron mass. At p_E, a δ function is placed, with a magnitude such that the GOS sum rules [10] are fulfilled. In order to get a rough estimate of the possible error produced by this method, I have compared calculations with PAI and GOS methods for Si. Results are shown in Table I, also see [3]. It is seen for $x = 26$ μm (equivalent to 4 cm of argon) that the most probable energy loss Δ_p is about 2% larger for PAI than for GOS, and the full-width-at-half maximum, w, is smaller for PAI than for GOS. For $x = 6.6$ μm Δ_p(PAI) is about 4% larger, while w differs by only 0.2%. The stopping power dE/dx is slightly larger for PAI. I expect similar differences for gases. A calculation of GOS for Ne and Ar would be quite easy, if tedious.

For the GOS calculation for Si, it may be noted that the difference between calculated and measured Δ_p and w is very close to 0 [3].

The photo absorption spectrum $\phi(hf)$ for argon is given in Figs. 1 and 2.

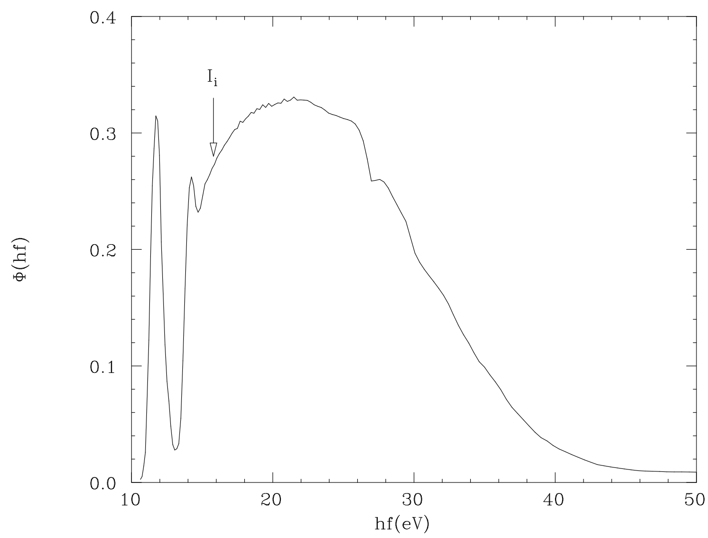

Figure 1: The photo absorption cross section $\phi(hf)$ for argon gas, linear scale.

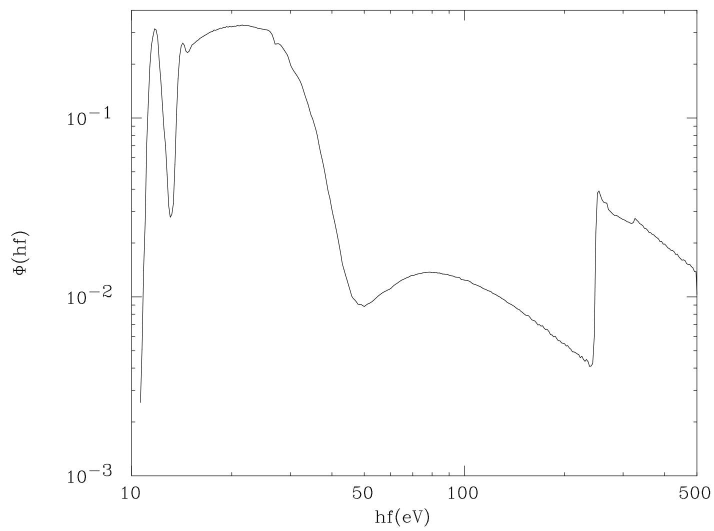

Figure 2: The photo absorption cross section $\phi(hf)$ for argon gas, log scales. The ionization threshold is about $I_i = 15.8$ eV. Since in this note the energy loss is considered, the excitations (below I_i) must be included in the calculation. In pure Ar, only the energy losses above I_i would contribute to the ionization. In the mixtures used in TPCs (usually including organic gases), excitations in Ar can produce ionization in the added gas. The threshold for L-shell excitations is about 250 eV.

The single collision spectrum calculated with PAI for 0.1 MeV electrons is shown in Fig. 3. It is similar to an energy loss spectrum measured with an electron microscope [11] (which is not shown here, a further study of this measured function is in progress). For comparison, the Rutherford single collision spectrum

$$\sigma_R(E) \;=\; \frac{2.55 \cdot 10^{-19}}{\beta^2} N_a \frac{Z}{A} \frac{1}{E^2} \quad eV\ cm^2 \tag{1}$$

used for the calculation of the Landau-Vavilov functions [1] is shown by the dashed line [4]. The single collision spectrum for 625 MeV/c pions differs little from that in Fig. 3. Modifications needed to include the effect of the methane in P-10 are small and not relevant for the present purpose.

III. Evolution of straggling functions $f(\Delta, x)$

Straggling functions are calculated with (Eq. (6.3) in [3])

$$f(x,\Delta) \;=\; \sum_{n=0}^{\infty} \frac{m^n e^{-m}}{n!} \sigma(\Delta)^{*n} \tag{2}$$

[1]In order to get the correct stopping power, the minimum energy loss for the Rutherford spectrum must be chosen as 0.1 eV, rather than the 10.75 eV used in PAI. The total collision cross section then is 3860/cm, rather than 73/cm obtained from PAI. This explains that PAI in Fig. 8 is much broader than the Vavilov function.

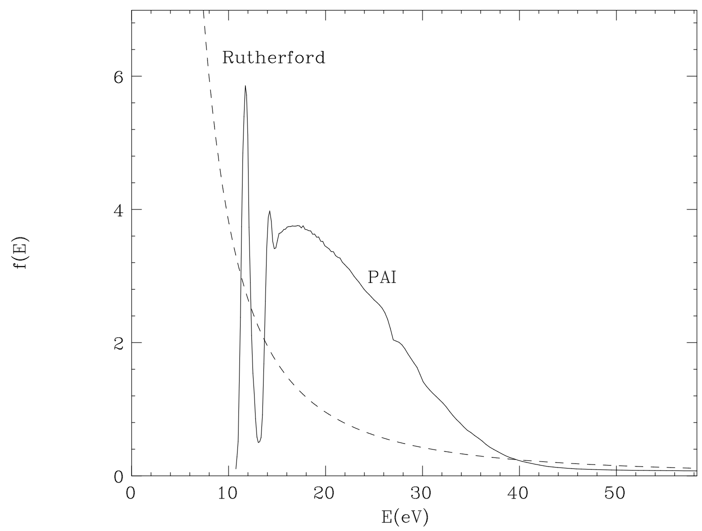

Figure 3: PAI energy loss function $f(E)$ for single collisions of 0.1 MeV electrons in Ar. The energy loss spectrum measured for these electrons in an electron microscope is fairly similar. The energy loss spectrum used for the Vavilov-Landau calculation, Eq. (1), is given by the dashed line. It is normalized to give the same stopping power as the PAI function.

where n is the number of collisions *one* particle experiences, $m = x \cdot M_0$ is the average number of collisions particles suffer in traversing a thickness x and

$$\sigma(\Delta)^{*n} \;=\; \int_0^{\Delta} \sigma(E) \cdot \sigma(\Delta)^{*(n-1)} \cdot (\Delta - E) \cdot dE \tag{3}$$

is the n-fold convolution of the single collision spectrum $\sigma(E)$. The moments of $\sigma(E)$ are

$$M_\nu = \int_0^{\infty} E^\nu \sigma(E) \cdot dE \qquad \nu = 0, 1, 2... \tag{4}$$

For singly charged particles with $\beta\gamma$ =4.48 (pions with momentum 625 MeV/c) the total collision cross section is $M_0 = 30.1$ collisions/cm and the stopping power is $M_1 = dE/dx = 2.555$ keV/cm. In the present context, M_2 is not relevant. In order to understand the features seen in the convoluted functions (Figs. 4-7), it is useful to know some of the partial integrals, σ_p, over $\sigma(E)$ (see Figs. 1,2 for the choices). For $E < 50$ eV, $\sigma_p = 26.5$/cm; $50 < E < 245$ eV, $\sigma_p = 1.9$/cm (this is up to the L-shell absorption edge); $E > 245$ eV, $\sigma_p = 1.7$/cm (includes all L- and K-shell excitations); $E > 3.2$ keV, $\sigma_p = 0.053$/cm (includes K-shell excitations). Thus, on the average, a K-shell excitation would only occur in segments 20 cm or longer. A narrow feature of the single collision spectrum will remain narrow in the convolutions with small n, e.g. the peak due to excitations at 11.7 eV is seen up to 2 mm, Fig. 6; two collisions with this loss (peak a) appear at 23 eV up to about 2 mm, but for $n = 3$ collisions, at 35 eV, the peak disappears in the background.

Broad features such as the "peak" between 13 and 40 eV in Fig. 3 are discernable as peak c in Figs. 4, 5, but have disappeared at 3 mm; instead peak d for $n \geq 2$ is dominant. The L-shell excitation at 250 eV in Fig. 2 is broadened by the concurrent excitations at lower energies, thus appears as a broad peak at e in Fig. 5 (for $x = 1.4$ mm, $m_L = 0.23$). It then increases and shifts to higher energies in Fig. 6 (on the average, $m_L = 1$ collision at 6 mm, but shifted to $\Delta \approx 700$ eV by the convolution with peak d). In Fig. 7, the changes in the peaks are indicated.

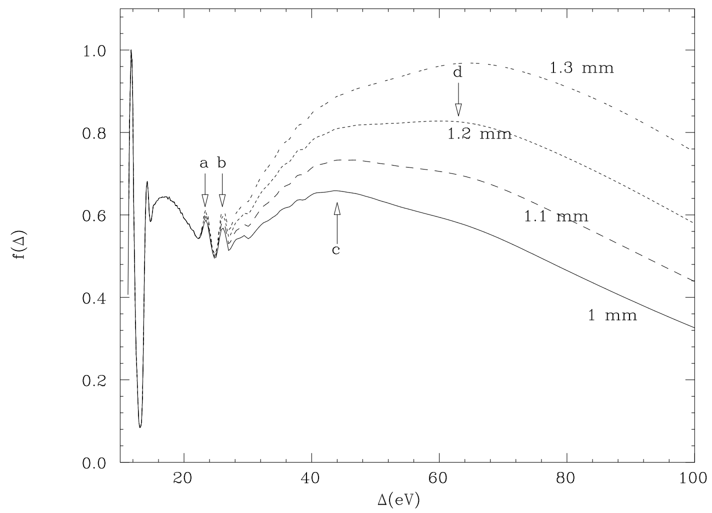

Figure 4: Straggling functions for singly charged particles with $\beta\gamma = 4.48$ (e.g. 625 MeV/c pions) traversing segments of length $x = 1.0$ to 1.3 mm in Ar. The total single collision cross-section is 30 collisions/cm. The functions are normalized to 1.0 at the most probable value (at 11.7 eV). The peaks a and b at 23 and 26 eV correspond to $n = 2$ collisions with 11.7 and 14 eV, see Eq. (2). The broad peak at 17 eV is due to single collisions, see Fig. 2. For 2 collisions it broadens and shifts to about 43 eV, marked c, and for $n = 3$ it can be seen at d. It may be noted that the peak at 11.7 eV (if the function is normalized to unit area) is exactly proportional to me^{-m}, as expected from Eq. (2). Energy losses to L-shell electrons of Ar, at 250 eV in Fig. 1b, are not shown here. They have an amplitude of 0.04. The $\delta-$function at $\Delta = 0$, $n = 0$, Eq. (2), is not shown. For $x = 1$ mm, it would be $e^{-m} = 0.05$.

Finally, at $x = 15$ mm, no separate features are discernible, and the function reaches the familiar "Landau-Vavilov" shape. The Vavilov function for $x = 15$ mm is compared to the PAI approximation in Fig. 8. It is much narrower than the PAI function, and would approach it only for $x \gg 1000$ cm, see Fig. 15 in [3].

IV. Conclusions.

The functions presented here demonstrate the extensive changes in the structure of the straggling functions with changing absorber thickness. In experimental measurements, several effects will modify the functions shown here:

a. Stochastic variations due to a finite number of particles (such as in an experiment) will be superimposed on the structure shown here.

b. The ionization measured in pure Ar will be caused only by energy losses above about 15.8 eV.

c. Usually, measurements will be made in a gas mixture. Then the excited states of Ar below 15.8 eV can lead to ionization of the molecules in the mixture [12].

d. "Noise" introduced by the gas multiplication process and the amplifiers will broaden the calculated straggling functions. The effect will be especially large for $x < 1$ cm. Also, the primary ionization function will be "grainy": each energy loss Δ will produce a small number of electron-ion pairs (on the average given by Δ/W, $W \approx 25$ eV), and the measured Δ must be located at multiples of 25 eV.

e. Ionization collection: $\delta-$rays can carry energy out of or into the counting volume.

Acknowledgments.

I am grateful to C. E. Brion for giving me the tables of photo absorption cross sections; and to P. Rez for discussions about the energy loss processes.

Table I. Comparison of properties of straggling functions $f(\Delta)$ calculated for $x = 26\ \mu$m of Si (equivalent to 4 cm of Ar) with Bethe-GOS and PAI methods. Given are most probable energy losses Δ_p(keV), the full-width-at half maximum w(keV) and the stopping power dE/dx(MeV/cm), as a function of $\beta\gamma$. Δ_p and w are the same for all particles, but dE/dx will depend on particle mass, see Table V in [3]. Note that the mean energy loss $< \Delta >= x \cdot dE/dx$ (last col.) is about twice as large as Δ_p, also see Table V in [3].

$\beta\gamma$	Δ_p		w		dE/x		$< \Delta >$
	GOS	PAI	GOS	PAI	GOS	PAI	
1	9.046	9.265	5.674	5.582	5.783	5.818	15.1
2	5.795	5.935	3.960	3.907	4.064	4.085	10.6
3	5.325	5.451	3.757	3.667	3.859	3.878	10
5	5.228	5.345	3.676	3.631	3.910	3.927	10.2
20	5.483	5.594	4.011	3.966	4.459	4.475	11.6
40	5.551	5.661	4.143	4.098	4.728	4.744	12.3
70	5.577	5.687	4.188	4.188	4.924	4.940	12.8
100	5.586	5.696	4.188	4.189	5.038	5.054	13.1

References

[1] M.Pfützner, H. Geissel, G. Münzenberg, F. Nickel, Ch. Scheidenberger, K.-H. Schmidt, K. Sümmerau, T. Brohm, B. Voss and H. Bichsel, Nucl Inst Meth **B 86** (1994) 213-218

[2] A. M. Kellerer, *Mikrodosimetrie*, (Strahlenbiologisches Institut der Universität München), G. S. F. Bericht B-1 (1968).

[3] Hans Bichsel, Rev. Mod. Phys. **60** (1988) 663.

[4] Hans Bichsel and Roberta P. Saxon Phys Rev **A 11**, 1286 (1975).

[5] W. W. M. Allison and J. H. Cobb, Annu. Rev. Nucl. Part. Sci. **30** (1980) 253.

[6] Pavel Newsky (Brookhaven Natl. Lab.), private communication (July 1999)

[7] Hans Bichsel, Section 87 in Atomic, molecular and optical physics handbook, G. Drake, ed., Amer. Inst. Phys. (1996)

[8] W. F. Chan, G. Cooper, X. Guo, G. R. Burton and C. E. Brion, Phys Rev **A 46**, 149 (1992).

[9] W. F. Marr, Atomic and Nuclear Data Tables **46**, 149 (1992).

[10] U. Fano, Annual Review of Nuclear Science **13**, 1 (1963).

[11] EELS atlas, C. C. Ahn and O. L. Krivanek, Gatan, Inc. Warrendale, PA and Center for Solid State Science, Arizona State University, Tempe, AZ (1983).

[12] "Atomic and molecular data for radiotherapy and radiation research", IAEA-TECDOC-799, International Atomic Energy Agency, May 1995

[13] Wolfgang Börsch-Supan, J. Research of the Nat. Bur. Stand.-B **65B**, 245 (1961).

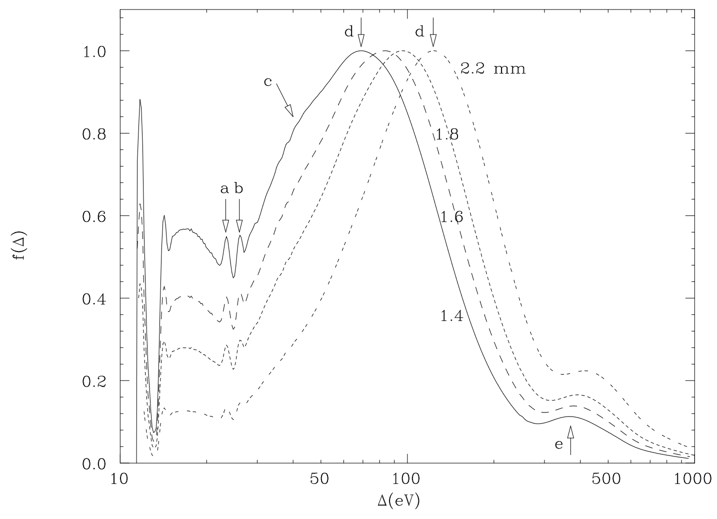

Figure 5: Similar to Fig. 4, for $x = 1.4$ to 2.2 mm. The most probable energy loss Δ_p at peak d is due to $n \geq 3$ collisions for $E < 40$ eV, and appears at 70 to 130 eV. The functions are normalized to 1.0 at that peak. The contributions at 10 to 30 eV become small. The change in Δ_p is not proportional to x. Contributions from collisions with L-shell electrons appear at e, with probability with probability increasing with x.

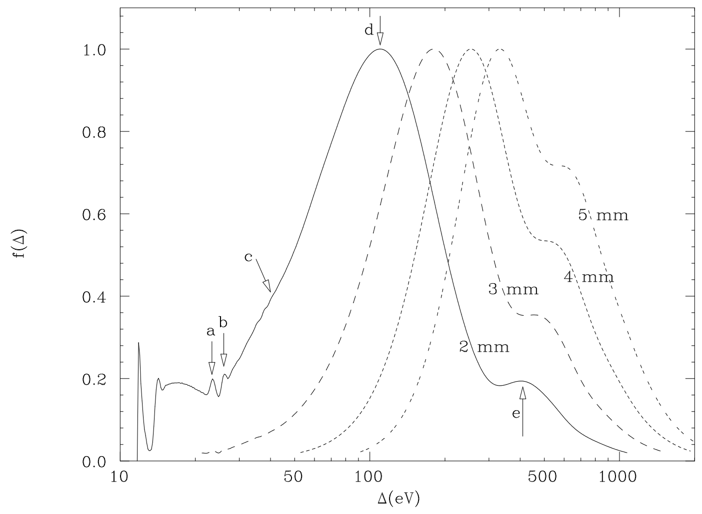

Figure 6: Similar to Fig. 5, for $x = 2$ to 5 mm. Peak c has disappeared, peak d is the dominant contribution and defines the most probable energy loss Δ_p. The buildup for peak e at 440 to 640 eV is the contribution from L-shell collisions. It appears roughly at 250 eV plus Δ_p. The total cross section for collisions with $E > 250$ eV is only 1.7 collisions/cm, thus the amplitude of the peak e is roughly proportional to x.

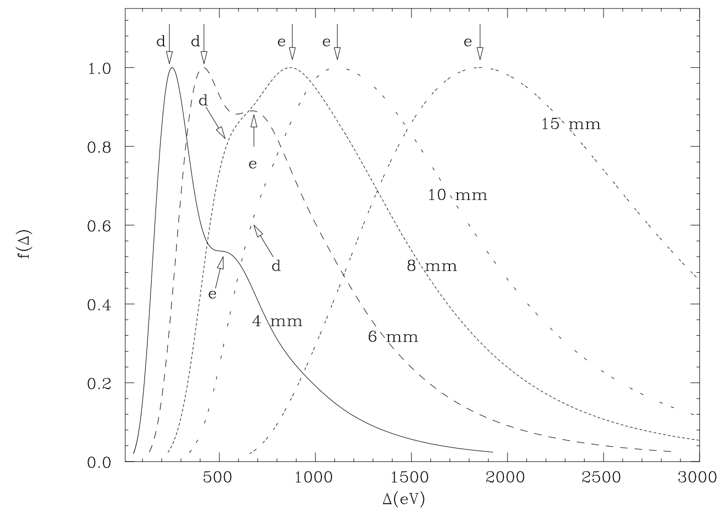

Figure 7: Similar to Fig. 4, for $x = 4$ to 15 mm. Peak d is dominant for $x = 4$ and 6 mm, but peak e due to L-shell collisions increases. It becomes the dominant feature at $x \geq 8$ mm, with a large shift of the most probable energy loss Δ_p from 400 eV to 850 eV. A shoulder of peak d, for multiple collisions for $E < 40$ eV remains, and is just perceptible at $x = 10$ mm. For $x = 15$ mm, the peaks have merged and the straggling function has reached the Vavilov shape, but see next Fig.

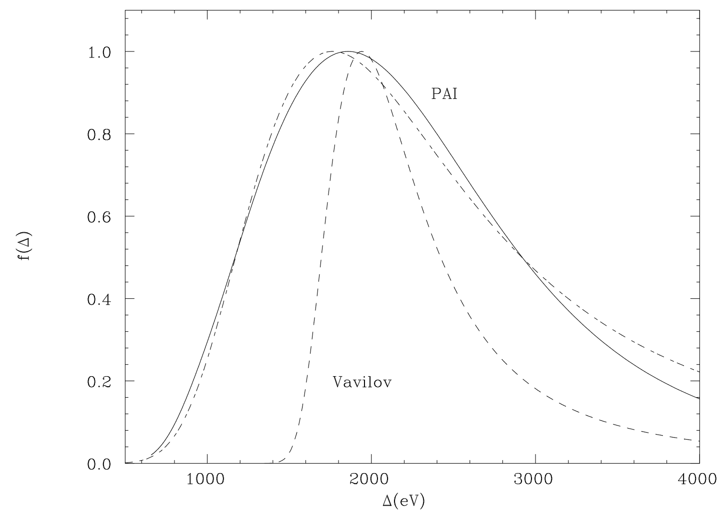

Figure 8: Comparison of the PAI and Vavilov energy loss functions function for $\beta\gamma = 4.48$ for 1.5 cm of Ar. For the PAI function, $\Delta_p = 1.86$ keV, $w = 1.75$ keV. The Vavilov function has the parameters $\xi = 0.181$ keV, $\kappa = 9.2 \cdot 10^{-6}$, $\Delta_p = 1.94$ keV, $w = 4.019 \cdot \xi = 0.72$ keV. Its width is less than half. This function differs by less than 1 in 10000 from the Landau function given by Börsch-Supan.